

(Scientific Note)

The Prediction Methods for the Sea Loads of a Catamaran Ship in Waves

MING-CHUNG FANG*, MING-LING LEE*, AND SHENG-FU YI**

*Department of Naval Architecture and Marine Engineering
National Cheng Kung University
Tainan, Taiwan, R.O.C.

**Department of Naval Architecture
National Kaoshiung Institute of Marine Technology
Kaoshiung, Taiwan, R.O.C.

(Received November 29, 1995; Accepted March 15, 1996)

ABSTRACT

Based on the strip theory, we propose a hybrid method to accurately predict the sea loads of a catamaran ship advancing in waves. Because the ship motion and sectional hydrodynamic coefficients are the primary factors affecting the sea loads, their corresponding mathematical models are derived, including the hydrodynamic interactions. With the corresponding forces on the ship hull, the sea loads on the mid-point of the cross deck can be obtained by using the free-free beam concept. Either a standard approach or a simplified approach normally solves such kinds of sea loads. However, instead of employing those approaches, we propose another method called hybrid approach. Such approach not only considers the different section shapes, but also includes the effects of pitch and yaw motions. Results obtained by hybrid method are preferable to those from the other approaches. Therefore, the hybrid approach proposed here can be considered as a highly effective tool in analyzing the sea loads for a catamaran ship in waves.

Key Words: sea loads, hydrodynamic, strip theory

1. Introduction

The catamaran ship generally has a larger weather deck, larger transverse stability and available flexible space between two hulls than the monohull ship. The catamaran ship is normally used for marine research expeditions, ocean mining, passenger transport and military purposes

Considering the catamaran ship's structural design requires calculating the wave loads. The wave loads include the vertical shear force, horizontal shear force, transverse vertical bending moment, lateral bending moment and vertical torsion moment. The magnitude of the corresponding wave load is closely related to the wave force and ship motions. Because the transverse span of the catamaran ship is generally large, damage usually occurs due to the wave action if the design is inadequate. Therefore, much emphasis for the wave loads of catamaran ship is placed on the cross deck's midspan which is different from that for a monohull ship.

Standard approach (Kim, 1976; Reilly *et al.*, 1988) and simplified approach (Lee *et al.*, 1973; Lee and Curphey, 1977) are the conventional methods for analyzing the wave loads. Instead of using the sectional pressure distribution, Kim (1976) used the sectional exciting force and hydrodynamic forces to calculate wave loads. Reilly *et al.* (1988) calculated the corresponding wave loads by using the integration of the sectional pressure. Lee *et al.* (1973) and Lee and Curphey (1977) assumed that the catamaran ship's section shape is uniform and symmetric for fore and aft. Therefore, the pitch motion and yaw motion are neglected and the action force on each section will be simplified. Consequently calculating the wave loads becomes relatively simple.

The standard approach, which must consider all regular procedures to calculate the wave loads, takes much more time than the simplified approach. However, the simplified approach merely uses one sectional shape to simulate the entire ship which will, subsequently lose the original characteristics of the ship and

somehow become impractical. In this study, we propose a hybrid method which combines the merits of the above approaches. By employing the proposing hybrid method, enhanced results can be attained for the transverse vertical bending moment and vertical torsion moment. Besides, the calculation time is also quite efficient.

The hydrodynamic coefficients used in this study are based on previous methods (Fang, 1985, 1987, 1988; Kim *et al.*, 1980). In those investigations, not only are the even and odd potentials treated separately but the hydrodynamic interactions are also considered. Owing to the above considerations, calculation accuracy for the wave loads and motions are improved.

An ASR catamaran ship is selected here as the calculation model. Also, the computer programs for the standard approach and hybrid method are developed to calculate the wave loads; those results are compared with those of Lee *et al.* (1973) which are calculated by simplified approach. The comparison reveals that the results obtained by the hybrid method more closely correlate with each other than those of the other two methods. Moreover the three methods and corresponding mathematical formulas are described in the subse-

quent sections.

II. Equations of Motions and Hydrodynamic Forces

The fact that calculating of sea loads is closely related to the ship's motion and hydrodynamic forces, necessitates that a mathematical model first be derived for these two factors. Figure 1 shows that the inertia and body coordinate systems are designated by O-XYZ and o-xyz, respectively. The ship's motion in response to the regular waves is calculated by solving the following five linear coupled equations if the surge motion is small and can be neglected:

$$\sum_{m=2}^6 [-\omega^2 (M + A_{mj}) - i\omega B_{mj} + C_{mj}] \xi_m = F_j \quad (1)$$

where A_{mj} , B_{mj} and C_{mj} represent the added mass, damping coefficient and restoring force, respectively; ξ_m denotes the motion response; F_j is the exciting force; M_o denotes the ship mass; subscripts m and j represent the mode of motion and direction of force, respectively; and mode m , $j=2, 3, 4, 5, 6$ represent sway(η), heave(ζ), roll(ϕ), pitch(ψ) and yaw(χ), respectively.

The sectional hydrodynamic forces, including the effects due to heave, sway and roll motions, can be calculated by solving two separated boundary value problems, i.e., diffraction problem and radiation problem. The diffraction problem is related to the wave exciting force while the radiation problem is related to the added mass and damping coefficients. Because the corresponding hydrodynamic coefficients have already been developed, we neglect the complicated procedures of derivation and the corresponding formulas can be found in previous literature (Kim, 1972; Yi, 1994).

III. Sea Loads

By considering only the linear theory, the sea loads for a ship advancing in waves arise from the following five components: (1) ship weight or ship

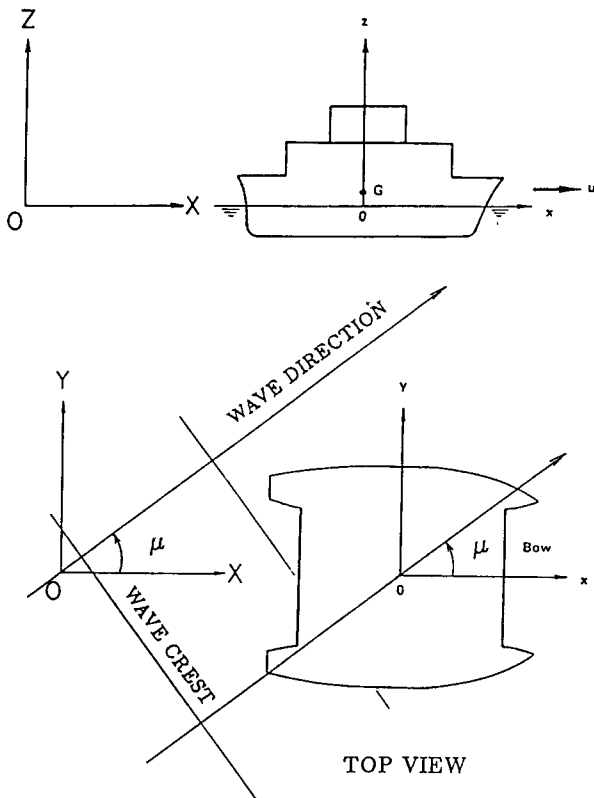


Fig. 1. Coordinate system.

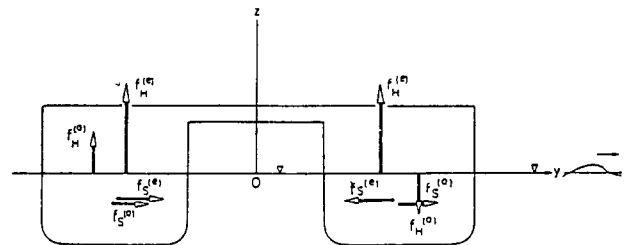


Fig. 2. Sectional exciting force due to the unit wave amplitude.

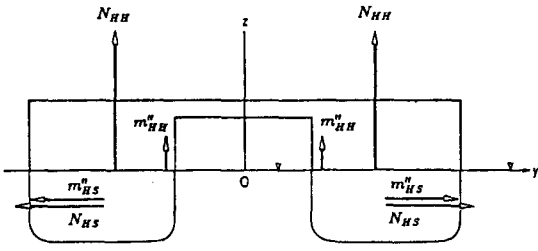


Fig. 3. Sectional hydrodynamic forces due to heave mode.

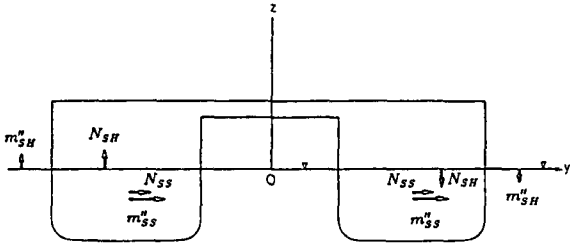


Fig. 4. Sectional hydrodynamic forces due to sway mode.

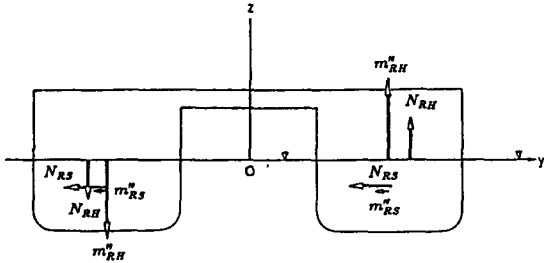


Fig. 5. Sectional hydrodynamic forces due to roll mode.

inertia force, (2) Froude-Krylov force due to incident wave, (3) diffraction force, (4) hydrodynamic inertia force, i.e., added mass, and damping force, and (5) restoring force. Figures 2-5 present the corresponding sectional hydrodynamic force, i.e., exciting force, added mass and damping coefficient, due to different motion modes.

Figure 2 presents the sectional exciting forces per unit wave amplitude denoted by f . Where superscripts o and e represent the odd and even functions, respectively, while subscripts H and S represent heave and sway modes, respectively. Also, Figs. 3-5 show the added mass forces (m'') and damping forces (N) due to the heave (H), sway (S) and roll (R) motions, respectively. The first subscript represents the motion mode, while the second subscript denotes the force mode's direction. In those figures, all forces are symmetrical except $f_H^{(o)}$, $f_S^{(e)}$, m''_{HS} , N_{HS} , m''_{SH} , N_{SH} , m''_{RS} , N_{RS} which are anti-symmetrical. When calculating the motions, the anti-symmetrical forces are

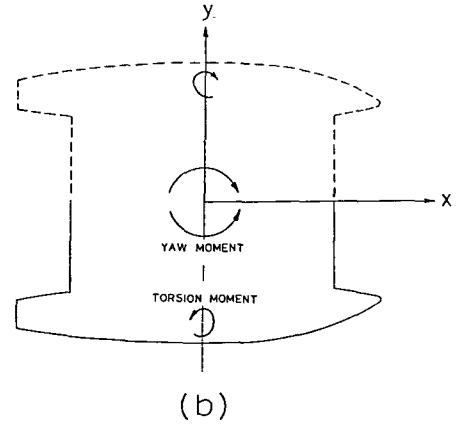
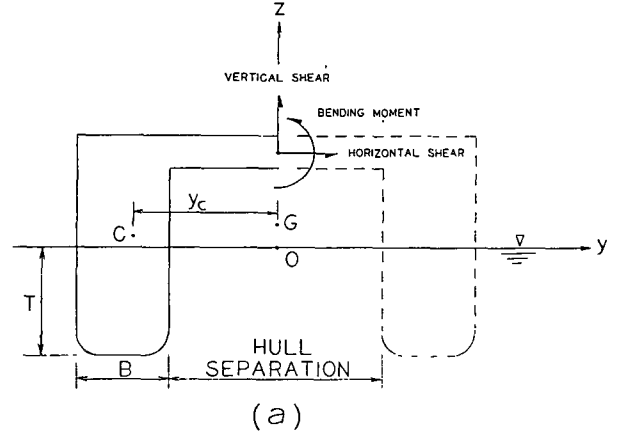


Fig. 6. The definition of sea loads for standard approach.

neglected because they cancel out each other. However, they can not be neglected when calculating the sea loads.

Figure 6 shows the corresponding sea loads considered in the catamaran ship's cross deck, i.e. vertical shear force, horizontal shear force, transverse vertical bending moment, yaw moment and torsion moment. Next, three calculation methods for the sea loads stated above are described as follows:

1. Standard Approach

The method is generally used to calculate sea loads. Here, we consider the ship hull as a free-free beam and take the free body diagram to calculate the sea loads by force equilibrium. By using the free body diagram in Fig. 6a, the formulas of the sectional sea loads can be derived in the midspan point of the cross deck located on the intersection of the longitudinal neutral axis and z axis. Next, the sectional values along the ship length can be integrated to obtain the sea loads for the entire ship. The corresponding formulas are

listed as below.

(1) Vertical shear force:

$$\begin{aligned}
 \frac{F_\zeta}{a} = & \int_{-\ell_1}^{\ell_2} f_H^{(o)+(e)}(x) dx \\
 & + \left[\int_{-\ell_1}^{\ell_2} \omega^2 m_o(x) (\zeta - x\psi + y_c\varphi) dx \right] \frac{1}{a} \\
 & + \left[\int_{-\ell_1}^{\ell_2} K_{HH}(x) dx - \int_{-\ell_1}^{\ell_2} b_H(x) dx \right] \frac{\zeta}{a} \\
 & + \left[\int_{-\ell_1}^{\ell_2} (-x) K_{HH}(x) dx + \int_{-\ell_1}^{\ell_2} x b_H(x) dx \right] \frac{\psi}{a} \\
 & + \left[\int_{-\ell_1}^{\ell_2} K_{SH}(x) dx \right] \frac{\eta}{a} + \left[\int_{-\ell_1}^{\ell_2} x K_{SH}(x) dx \right] \frac{\chi}{a} \\
 & + \left[\int_{-\ell_1}^{\ell_2} K_{RH}(x) dx - \int_{-\ell_1}^{\ell_2} b_H(x) y_f dx \right] \frac{\varphi}{a} \quad (2)
 \end{aligned}$$

(2) Horizontal shear force:

$$\begin{aligned}
 \frac{F_\eta}{a} = & \int_{-\ell_1}^{\ell_2} f_S^{(o)+(e)}(x) dx \\
 & + \left[\int_{-\ell_1}^{\ell_2} \omega^2 m_o(x) (\eta + x\chi + \overline{CG}\varphi) dx \right] \frac{1}{a} \\
 & + \left[\int_{-\ell_1}^{\ell_2} K_{SS}(x) dx \right] \frac{\eta}{a} + \left[\int_{-\ell_1}^{\ell_2} x K_{SS}(x) dx \right] \frac{\chi}{a} \\
 & + \left[\int_{-\ell_1}^{\ell_2} K_{RS}(x) dx \right] \frac{\varphi}{a} + \left[\int_{-\ell_1}^{\ell_2} K_{HS}(x) dx \right] \frac{\zeta}{a} \\
 & + \left[\int_{-\ell_1}^{\ell_2} (-x) K_{HS}(x) dx \right] \frac{\psi}{a} \quad (3)
 \end{aligned}$$

(3) Transverse vertical bending moment:

$$\begin{aligned}
 \frac{M_\varphi}{a} = & \left\{ \int_{-\ell_1}^{\ell_2} f_H^{(o)+(e)}(x) dx \right. \\
 & + \left[\int_{-\ell_1}^{\ell_2} \omega^2 m_o(x) (\zeta - x\psi + y_c\varphi) dx \right] \frac{1}{a} \\
 & + \left[\int_{-\ell_1}^{\ell_2} K_{HH}(x) dx - \int_{-\ell_1}^{\ell_2} b_H(x) dx \right] \frac{\zeta}{a} \\
 & + \left[\int_{-\ell_1}^{\ell_2} (-x) K_{HH}(x) dx + \int_{-\ell_1}^{\ell_2} x b_H(x) dx \right] \frac{\psi}{a}
 \end{aligned}$$

$$\begin{aligned}
 & + \left[\int_{-\ell_1}^{\ell_2} K_{SH}(x) dx \right] \frac{\eta}{a} + \left[\int_{-\ell_1}^{\ell_2} x K_{SH}(x) dx \right] \frac{\chi}{a} \\
 & + \left[\int_{-\ell_1}^{\ell_2} K_{RH}(x) dx - \int_{-\ell_1}^{\ell_2} b_H(x) y_f dx \right] \frac{\varphi}{a} \} \cdot |y_g| \\
 & - \left\{ \left[\int_{-\ell_1}^{\ell_2} \omega^2 m_o(x) (\eta + x\chi + \overline{CG}\varphi) dx \right] \frac{1}{a} \right\} \cdot (\overline{CG} + \overline{GS}) \\
 & - \left\{ \int_{-\ell_1}^{\ell_2} f_S^{(o)+(e)}(x) dx + \left[\int_{-\ell_1}^{\ell_2} K_{SS}(x) dx \right] \frac{\eta}{a} \right. \\
 & + \left[\int_{-\ell_1}^{\ell_2} x K_{SS}(x) dx \right] \frac{\chi}{a} + \left[\int_{-\ell_1}^{\ell_2} K_{RS}(x) dx \right] \frac{\varphi}{a} \\
 & + \left[\int_{-\ell_1}^{\ell_2} K_{HS}(x) dx \right] \frac{\zeta}{a} + \left[\int_{-\ell_1}^{\ell_2} (-x) K_{HS}(x) dx \right] \frac{\psi}{a} \} \\
 & \cdot (\overline{z} + \overline{OS}) \quad (4)
 \end{aligned}$$

(4) Torsion moment:

$$\begin{aligned}
 \frac{M_\psi}{a} = & \int_{-\ell_1}^{\ell_2} (-x) f_H^{(o)+(e)}(x) dx \\
 & - \left[\int_{-\ell_1}^{\ell_2} \omega^2 m_o(x) (\zeta - x\psi + y_c\varphi) x dx \right] \frac{1}{a} \\
 & + \left[\int_{-\ell_1}^{\ell_2} (-x) K_{HH}(x) dx + \int_{-\ell_1}^{\ell_2} x b_H(x) dx \right] \frac{\zeta}{a} \\
 & + \left[\int_{-\ell_1}^{\ell_2} x^2 K_{HH}(x) dx - \int_{-\ell_1}^{\ell_2} x^2 b_H(x) dx \right] \frac{\psi}{a} \\
 & + \left[\int_{-\ell_1}^{\ell_2} (-x) K_{SH}(x) dx \right] \frac{\eta}{a} \\
 & + \left[\int_{-\ell_1}^{\ell_2} (-x^2) K_{SH}(x) dx \right] \frac{\chi}{a} \\
 & + \left[\int_{-\ell_1}^{\ell_2} (-x) K_{RH}(x) dx + \int_{-\ell_1}^{\ell_2} x b_H(x) y_f dx \right] \frac{\varphi}{a} \quad (5)
 \end{aligned}$$

(5) Yaw moment:

$$\begin{aligned}
 \frac{M_\chi}{a} = & \int_{-\ell_1}^{\ell_2} x f_S^{(o)+(e)}(x) dx \\
 & + \left[\int_{-\ell_1}^{\ell_2} \omega^2 m_o(x) (\eta + x\chi + \overline{CG}\varphi) x dx \right] \frac{1}{a}
 \end{aligned}$$

$$\begin{aligned}
& + \left[\int_{-\ell_1}^{\ell_2} x K_{SS}(x) dx \right] \frac{\eta}{a} + \left[\int_{-\ell_1}^{\ell_2} x^2 K_{SS}(x) dx \right] \frac{\chi}{a} \\
& + \left[\int_{-\ell_1}^{\ell_2} x K_{RS}(x) dx \right] \frac{\phi}{a} + \left[\int_{-\ell_1}^{\ell_2} x K_{HS}(x) dx \right] \frac{\zeta}{a} \\
& \vdots \\
& + \left[\int_{-\ell_1}^{\ell_2} (-x^2) K_{HS}(x) dx \right] \frac{\psi}{a}
\end{aligned} \quad (6)$$

where

$$K_{HH}(x) = \omega^2 m_{HH}''(x) + i\omega N_{HH}(x)$$

$$K_{SH}(x) = \omega^2 m_{SH}''(x) + i\omega N_{SH}(x)$$

$$K_{RH}(x) = \omega^2 m_{RH}''(x) + i\omega N_{RH}(x)$$

$$K_{SS}(x) = \omega^2 m_{SS}''(x) + i\omega N_{SS}(x)$$

$$K_{RS}(x) = \omega^2 m_{RS}''(x) + i\omega N_{RS}(x)$$

$$K_{HS}(x) = \omega^2 m_{HS}''(x) + i\omega N_{HS}(x)$$

The above sea loads are expressed by per unit wave amplitude. Where y_c is the horizontal distance of the centroid of the half section; while y_f is the horizontal distance of the midpoint of water line of the half section; m_o is the half sectional mass; b_H is the restoring force per unit displacement; $\overline{CG} = \overline{OG} - z_c$ and z_c is the vertical position of the half section gravitational center; y_g is the horizontal position of the center of gravity for the half-side ship hull; \bar{z} is the vertical distance of the pressure center which may be replaced by the center of buoyancy due to the small amplitude; \overline{OS} is the vertical distance between waterline and longitudinal neutral axis of the cross deck; and \overline{GS} is the distance from the center of gravity to the longitudinal neutral axis of the cross deck. The torsion moment is taken about the axis parallel to y -axis and passes through S point, i.e., the intersection of the longitudinal neutral axis and the z -axis. Finally, the yaw moment is the moment around the z -axis due to the lateral force.

2. Simplified Approach

The simplified approach involves transferring the original catamaran ship to another two-dimensional ship with the original midship section and the same displacement. Therefore, the ship length is changed to an equivalent length to maintain the displacement constant. Another assumption is that the wave is limited in beam wave.

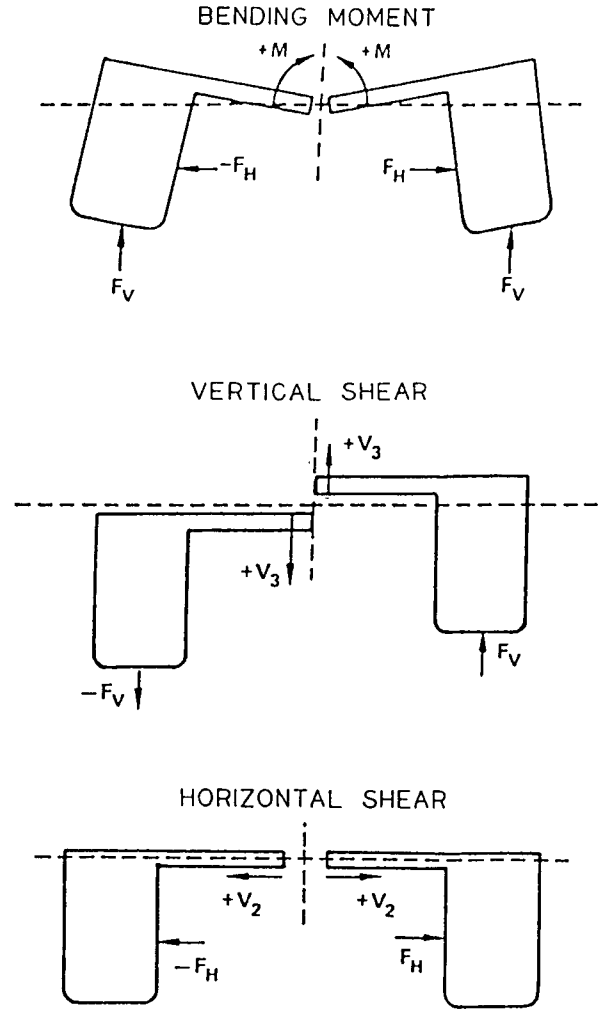


Fig. 7. The definition of sea loads for simplified approach

Owing to the symmetry of the fore and aft parts of the ship, only heave, roll and sway motions exist in the beam wave. Calculating the sea loads can be simplified by considering only the three modes of motions. Figure 7 provides the definition of the sea loads of the whole section (Lee *et al.*, 1973, Lee and Curphey, 1977). Previous literature describes the detail procedures (Lee *et al.*, 1973, Lee and Curphey, 1977) and are, therefore, neglected here. By using the corresponding force diagrams in Figs. 3-5, the following formulas for sea loads can be derived as,

(1) Vertical shear force:

$$\frac{F_V}{a} = \{ f_H^{(o)} + (\omega^2 m_o y_c) \phi / a + [\omega^2 m_{SH}'' + i\omega N_{SH}] \eta / a$$

$$+ [\omega^2 m''_{RH} + i\omega N_{RH} - b_H \cdot y_f] \varphi / a \} \cdot L_e \quad (7)$$

(2) Horizontal shear force:

$$\frac{F_\eta}{a} = \{ f_S^{(e)} + [\omega^2 m''_{HS} + i\omega N_{HS}] \zeta / a \} \cdot L_e \quad (8)$$

(3) Transverse vertical bending moment:

$$\begin{aligned} \frac{M_\varphi}{a} = & \{ \{ f_H^{(e)} + [(\omega^2 m''_{HH} + i\omega N_{HH}) \\ & - b_H + \omega^2 m_o] \zeta / a \} \cdot |y_c| \\ & - \{ f_S^{(e)} + [\omega^2 m''_{HS} + i\omega N_{HS}] \zeta / a \} \cdot (\bar{z}_p + \bar{OS}) \} \cdot L_e \end{aligned} \quad (9)$$

where L_e is the equivalent ship length.

Comparing the standard approach with the simplified approach reveals that the latter makes the formulas relatively simple and saves much computational time. However, it can not calculate the torsion moment and yaw moment because of the omission of the pitch and yaw motions. Results obtained from the simplified approach may also be worse than those of the standard approach.

3. Hybrid Approach

Although the simplified approach is quite simple, the ship configuration has been changed and the wave direction is also limited only in the beam wave. It is therefore somewhat impractical and the results have been proved to have some discrepancies. Practically, the pitch and yaw motions exist and contribute to the sea loads. The proposed hybrid approach combines the merits of the standard and simplified approaches. Because the hull body is floating in water, the wave loads in the midpoint of the transverse deck do not need to be calculated using the half free body diagram as the standard approach stipulates. We can consider the entire twin-hull free body diagram and some symmetrical and asymmetrical forces can be neglected as shown in the following formulas. Besides, we consider the real section shapes along the ship length and the five modes of motions including heave, sway, roll, pitch and yaw are considered. Restated, we simply add the effect of the pitch and yaw motions in the simplified approach. Consequently, the corresponding formulas can be written as

(1) Vertical shear force:

$$\frac{F_z}{a} = \int_{-\ell_1}^{\ell_2} f_H^{(o)}(x) dx + [\int_{-\ell_1}^{\ell_2} \omega^2 m_o(x) y_c dx] \frac{\varphi}{a}$$

$$+ [\int_{-\ell_1}^{\ell_2} K_{SH}(x) dx] \frac{\eta}{a} + [\int_{-\ell_1}^{\ell_2} x K_{SH}(x) dx] \frac{\chi}{a}$$

$$+ [\int_{-\ell_1}^{\ell_2} K_{RH}(x) dx - \int_{-\ell_1}^{\ell_2} b_H(x) y_f dx] \frac{\varphi}{a} \quad (10)$$

(2) Horizontal shear force:

$$\begin{aligned} \frac{F_\eta}{a} = & \int_{-\ell_1}^{\ell_2} f_S^{(e)}(x) dx + [\int_{-\ell_1}^{\ell_2} K_{HS}(x) dx] \frac{\zeta}{a} \\ & + [\int_{-\ell_1}^{\ell_2} (-x) K_{HS}(x) dx] \frac{\psi}{a} \end{aligned} \quad (11)$$

(3) Transverse vertical bending moment:

$$\begin{aligned} \frac{M_\varphi}{a} = & \{ \int_{-\ell_1}^{\ell_2} f_H^{(e)}(x) dx + [\int_{-\ell_1}^{\ell_2} K_{HH}(x) dx \\ & - \int_{-\ell_1}^{\ell_2} b_H(x) dx] \frac{\zeta}{a} \\ & + [\int_{-\ell_1}^{\ell_2} (-x) K_{HH}(x) dx + \int_{-\ell_1}^{\ell_2} x b_H(x) dx] \frac{\psi}{a} \\ & + [\int_{-\ell_1}^{\ell_2} \omega^2 m_o(x) (\zeta - x\psi) dx] \frac{1}{a} \} \cdot |y_g| \\ & - \{ \int_{-\ell_1}^{\ell_2} f_S^{(e)}(x) dx + [\int_{-\ell_1}^{\ell_2} K_{HS}(x)] \frac{\zeta}{a} \\ & + [\int_{-\ell_1}^{\ell_2} (-x) K_{HS}(x) dx] \frac{\psi}{a} \} \cdot (\bar{z} + \bar{OS}) \end{aligned} \quad (12)$$

(4) Torsion moment:

$$\begin{aligned} \frac{M_\psi}{a} = & \int_{-\ell_1}^{\ell_2} (-x) f_H^{(o)}(x) dx - [\int_{-\ell_1}^{\ell_2} x \omega^2 m_o(x) y_c dx] \frac{\varphi}{a} \\ & + [\int_{-\ell_1}^{\ell_2} (-x) K_{SH}(x) dx] \frac{\eta}{a} \\ & + [\int_{-\ell_1}^{\ell_2} (-x^2) K_{SH}(x) dx] \frac{\chi}{a} \\ & + [\int_{-\ell_1}^{\ell_2} (-x) K_{RH}(x) dx \\ & + \int_{-\ell_1}^{\ell_2} x b_H(x) y_f dx] \frac{\varphi}{a} \end{aligned} \quad (13)$$

(5) Yaw moment:

$$\begin{aligned} \frac{M_y}{a} = & \int_{-\ell_1}^{\ell_2} x f_S^{(e)}(x) dx + \left[\int_{-\ell_1}^{\ell_2} x K_{HS}(x) dx \right] \frac{\zeta}{a} \\ & + \left[\int_{-\ell_1}^{\ell_2} (-x^2) K_{HS}(x) dx \right] \frac{\psi}{a} \end{aligned} \quad (14)$$

Results in this study indicate that the formulas derived for the proposed hybrid approach are simpler than those of the standard one. $f_H^{(e)}$ and the hydrodynamic forces and inertia forces due to heave and pitch have been omitted in the Eqs. (10) and (13) if Eqs. (2) and (5) are compared. $f_S^{(o)}$ and the hydrodynamic forces and inertia forces due to sway, roll and yaw are omitted in Eqs. (11) and (14) if Eqs. (3) and (6) are compared. Comparing Eq. (12) with Eq. (4) reveals that $f_H^{(o)}$, $f_S^{(o)}$ and the hydrodynamic forces and the inertia forces due to sway, roll and yaw are omitted. Comparing the formulas for simplified approach with those of the proposed hybrid approach indicates that the latter is more rigorous.

Therefore, the hybrid approach obviously has the merits of the other two.

IV. Results and Discussion

Here, the ASR catamaran ship is selected as the model when calculating the sea loads. Table 1 presents the principal dimensions of the catamaran ship. Because the prediction accuracy of the ship motion affects the results of sea loads, the motion prediction is first investigated by comparing with the experimental results (Wahab *et al.*, 1971).

Table 1. Principal Dimensions of ASR Catamaran Model

Model No.		5061
Displacement, long tons in S.W.	(LT)	2794
Length (D.W.L.), L	(M)	64
Beam (each hull) at Waterline, B	(M)	7.32
Beam (overall), B_m	(M)	26.21
Draft at Midship, T	(M)	5.49
Hull Separation	(M)	11.58
Longitudinal Center of Gravity aft of F.P.	(M)	32.16
Vertical C.G., KG	(M)	6.4
Transverse Metacentric Height, GM	(M)	17.98
Radius of Gyration for Pitch	(M)	0.25L
Radius of Gyration for Roll	(M)	9.88
Vertical Distance of the Neutral Axis, $\bar{G}\bar{S}$ above the VCG	(M)	6.1
Transverse Distance of the C.G. of the Starboard Hull from G , y_g	(M)	8.99
Hull Separation/Beam		1.58
Model Scale Ratio		1/16.89

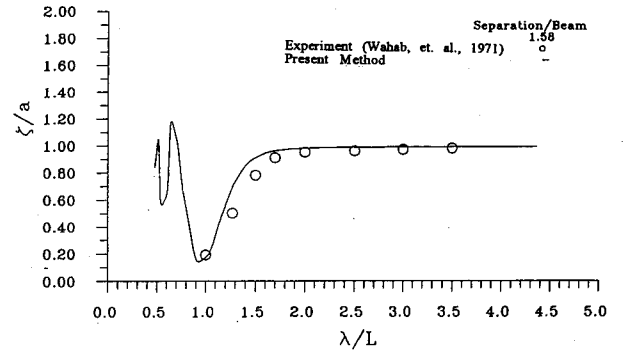


Fig. 8. The heave motion of ASR catamaran ship in beam wave with $Fn=0.1$.

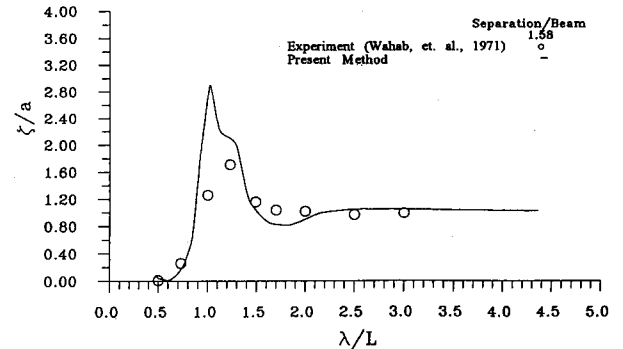


Fig. 9. The heave motion of ASR catamaran ship at $\mu=120^\circ$ with $Fn=0.31$.

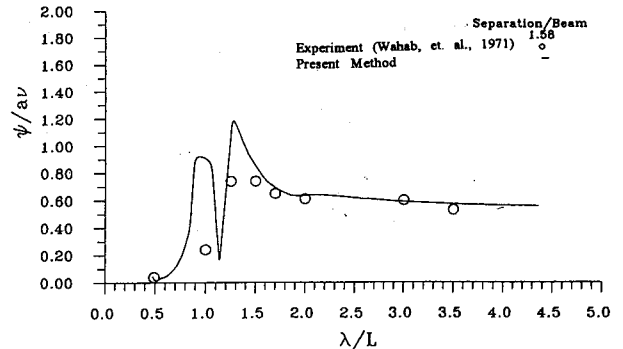


Fig. 10. The pitch motion of ASR catamaran ship at $\mu=120^\circ$ with $Fn=0.31$.

Figures 8-13 show the motions of ASR catamaran ship at different speeds in different waves. The results are expressed by nondimensional motion amplitude vs. λ/L . Figure 8 shows the heave motion in beam waves with ship speed $Fn=0.1$. The agreements are quite satisfactory. The results in Fig. 9 are the heave motion at $\mu=120^\circ$ with ship speed $Fn=0.31$. Similarly the results closely correspond to the experimental data.

Sea Loads of Catamaran Ship in Waves

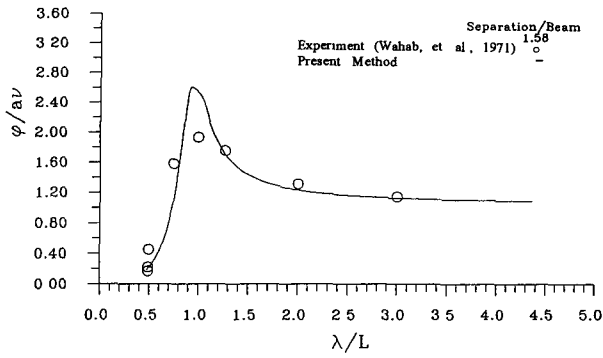


Fig. 11. The roll motion of ASR catamaran ship in beam wave with $F_n=0.0$.

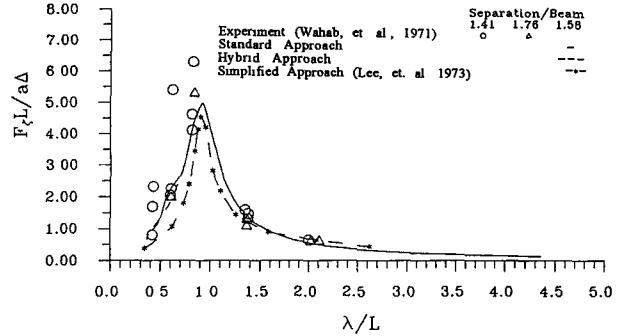


Fig. 14. The vertical shear force on the mid-point of cross deck in beam wave with $F_n=0.0$.

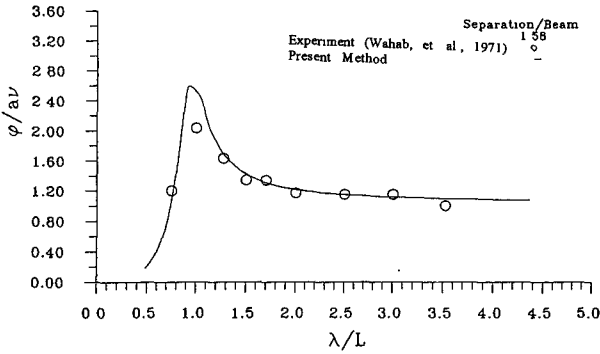


Fig. 12. The roll motion of ASR catamaran ship in beam wave with $F_n=0.1$.

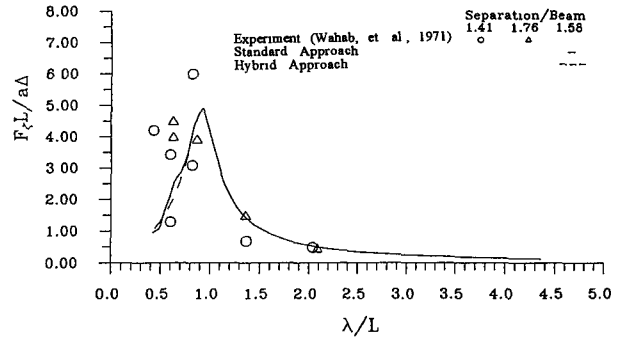


Fig. 15. The vertical shear force on the mid-point of cross deck in beam wave with $F_n=0.253$.

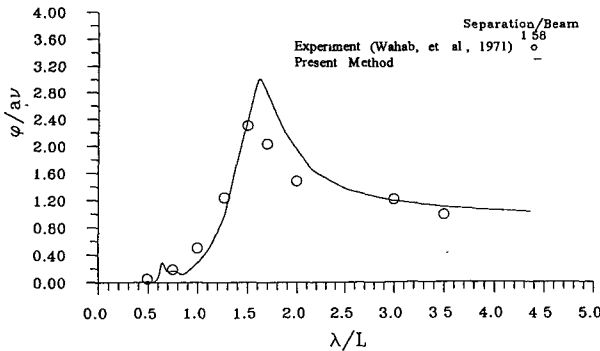


Fig. 13. The roll motion of ASR catamaran ship at $\mu=120^\circ$ with $F_n=0.31$.

the simplified approach are adopted here. Also, Figs. 14-28 compare the three sets of theoretical results with the experimental data (Wahab *et al.*, 1971). Two ship speeds ($F_n=0.0, 0.253$) and two wave headings ($\mu=90^\circ, 120^\circ$) are also considered. The sea loads considered are concentrated on the midpoint of the cross deck for the ASR catamaran ship. Figures 14 and 15 show the

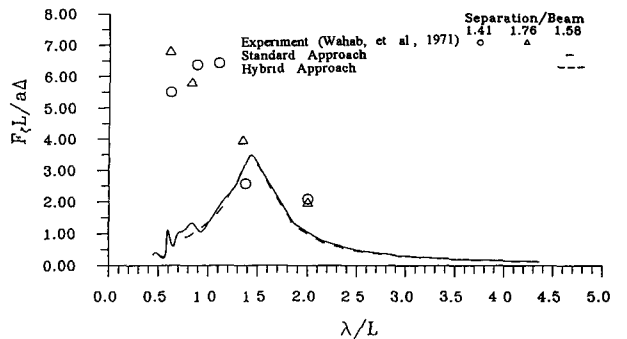


Fig. 16. The vertical shear force on the mid-point of cross deck at $\mu=120^\circ$ with $F_n=0.253$.

Figure 10 summarizes the results for pitch motion in bow waves, while Figs. 11-13 show the roll motion results for different wave headings. Generally, the comparisons are quite good and thereby confirm the following results for sea loads.

Here, the programs for the standard approach and hybrid approach are developed to calculate the corresponding sea loads. Results of Lee *et al.* (1973) for

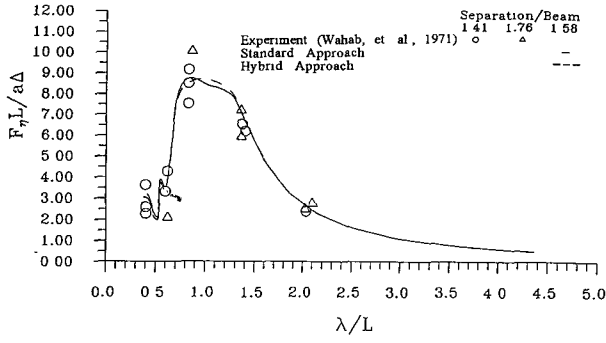


Fig. 17. The horizontal shear force on the mid-point of cross deck in beam wave with $Fn=0.0$.

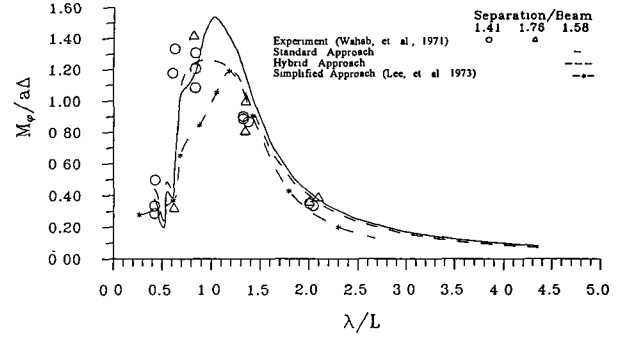


Fig. 20. The transverse vertical bending moment on the mid-point of cross deck in beam wave with $Fn=0.0$.

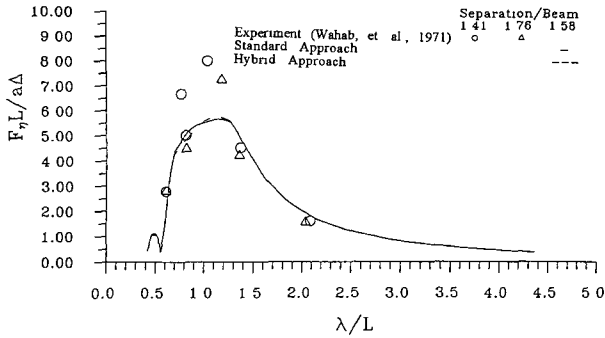


Fig. 18. The horizontal shear force on the mid-point of cross deck at $\mu=120^\circ$ with $Fn=0.0$.

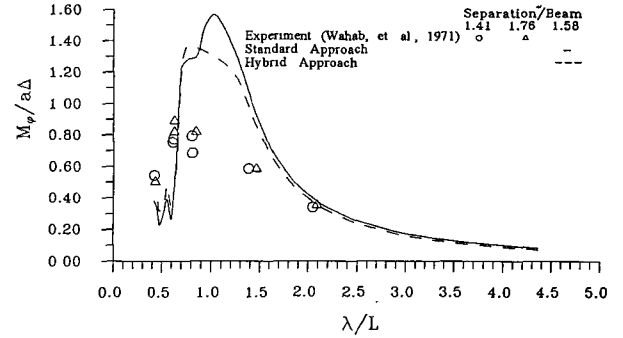


Fig. 21. The transverse vertical bending moment on the mid-point of cross deck in beam wave with $Fn=0.253$.

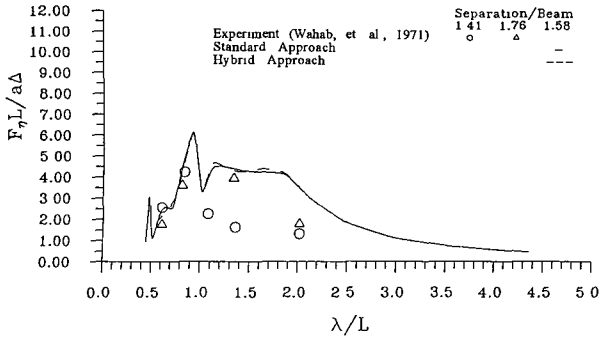


Fig. 19. The horizontal shear force on the mid-point of cross deck at $\mu=120^\circ$ with $Fn=0.253$.

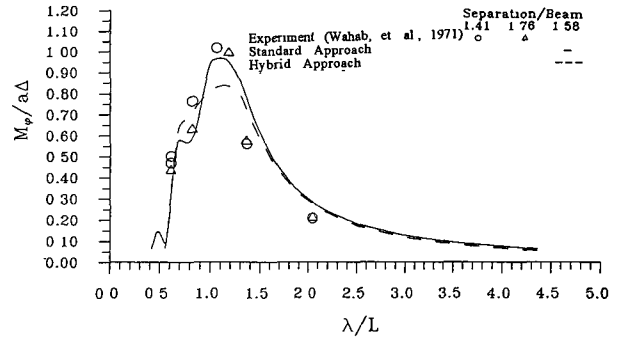


Fig. 22. The transverse vertical bending moment on the mid-point of cross deck at $\mu=120^\circ$ with $Fn=0.0$.

vertical shear force in the midpoint of the deck of the catamaran ship in beam waves. Results obtained from standard approach and hybrid approach closely correspond to the experimental data while those obtained by the simplified one are lower (Fig. 14). If the speed is included, i.e., Fig. 15, the results are similar to those in Fig. 14. Figure 16 summarizes the results for $\mu=120^\circ$ with speed effect. The theoretical results are generally

underestimated if the experimental data are compared.

Figures 17-19 show the horizontal shear forces in the midpoint of the deck. For zero speed cases in Figs. 17 and 18, the theoretical results are still satisfactory for both approaches. However, both theoretical results are overestimated in the long waves if the speed is considered as shown in Fig. 19.

Figures 20-23 display the results for the trans-

Sea Loads of Catamaran Ship in Waves

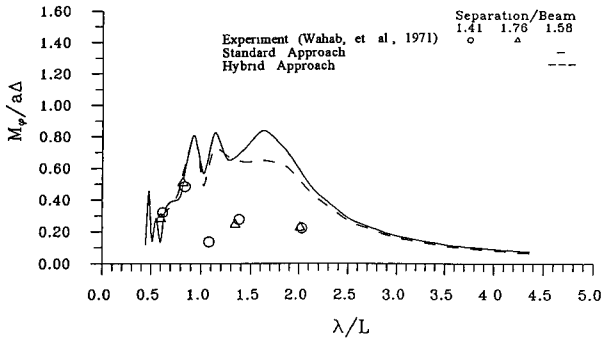


Fig. 23. The transverse vertical bending moment on the mid-point of cross deck at $\mu=120^\circ$ with $Fn=0.253$.

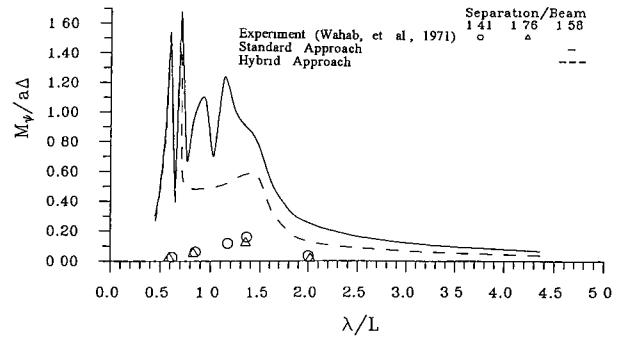


Fig. 25. The torsion moment on the mid-point of cross deck at $\mu=120^\circ$ with $Fn=0.253$.

verse vertical bending moment in the midpoint of the deck of the catamaran ship. For the beam wave case with zero speed as shown in Fig. 20, the hybrid approach correlates with the experimental data better than the standard approach whereas the simplified approach is the worst one. With the speed effect in Fig. 21, the hybrid approach and standard approach have a similar trend; however, the hybrid one is slightly better than the standard one if the experimental data are compared. For $\mu=120^\circ$ with a zero speed in Fig. 22, both theoretical results closely correspond to the experimental data. However, the standard approach is better than the hybrid one around the peak values while it is better for the hybrid approach in longer waves. Figure 23 presents the case with $Fn=0.253$. Although two theoretical approaches are generally overestimated in longer waves, the hybrid approach is still better than the standard one.

Figures 24 and 25 display the results for torsion moment. From Fig. 24, i.e., beam waves, the hybrid approach generally agrees with the experiment better than the standard one. For another wave heading, i.e., $\mu=120^\circ$, both theoretical results are overestimated;

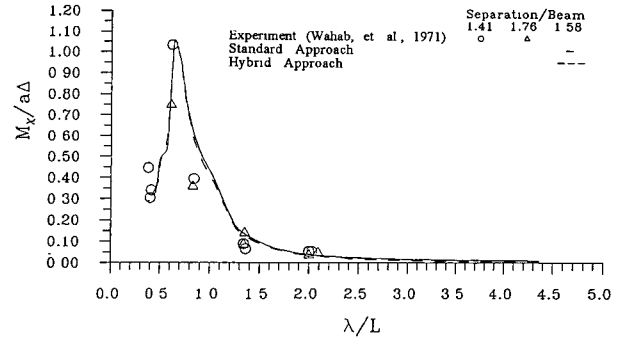


Fig. 26. The yaw moment on the mid-point of cross deck in beam wave with $Fn=0.0$.

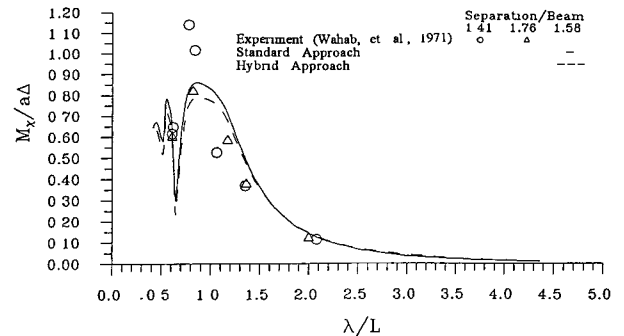


Fig. 27. The yaw moment on the mid-point of cross deck at $\mu=120^\circ$ with $Fn=0.0$.

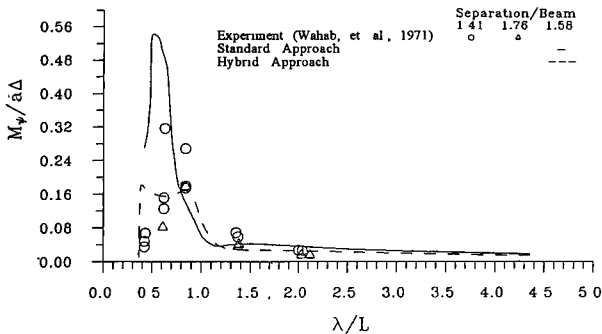


Fig. 24. The torsion moment on the mid-point of cross deck in beam wave with $Fn=0.0$.

however, the hybrid approach is still better than the standard one (Fig. 25).

Figures 26-28 summarize the results for the yaw moment. As indicated in those figures, the theoretical predictions are generally satisfactory for both approaches.

The effect of the motions on the sea loads is quite obvious, as indicated from a comparison of the corresponding results mentioned above particularly around

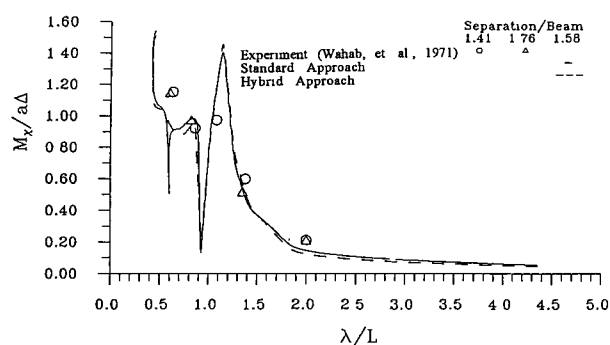


Fig. 28. The yaw moment on the mid-point of cross deck at $\mu=120^\circ$ with $Fn=0.253$.

the motions resonance, i.e., $\lambda/L=0.5-1.5$.

V. Conclusion

Based on the two-dimensional strip theory, we have proposed a mathematical model to calculate the ship motions and sea loads. A series of analyses have also been made for the different approaches and experimental data. Based on those results, we can conclude the following:

- (1) The motion predictions for the ASR catamaran ship in waves are generally satisfactory and closely related to the sea loads, thereby confirming the validity of the present strip theory.
- (2) General comparisons with the experimental results indicate that the hybrid approach developed here is the preferable one in accurately predicting the sea loads for a catamaran ship in waves. The hybrid approach combines the advantages of standard approach and simplified approach, i.e., less computational time and more accurate results.
- (3) The sea loads in the midpoint of the cross deck for the ASR catamaran can be accurately predicted for the zero speed in beam waves. Practically, the maximum sea loads for the catamaran generally occur in the zero speed condition in beam waves. Therefore, the technique developed here can be practically used for the cross deck structural design of the catamaran ship.
- (4) Some discrepancies still arise, particularly in bow waves. This may be owing to the three-dimensional effect which is to be studied in our near future work.

Acknowledgment

The authors would like to thank the National Science Council of the Republic of China for financial support of the project under the grant No. NSC 82-0403-E006-277.

Nomenclature

a	: incident wave amplitude
b_H	: sectional a restoring force per unit displacement
B	: beam of monohull
B_m	: beam of twin hull
F_n	: Froude number $(U/(gL)^{1/2})$
g	: acceleration of gravity
L	: ship length
L_e	: equivalent ship length
U	: ship speed
λ	: wave length
μ	: wave direction
ρ	: water density
ω_o	: wave frequency
ω	: encounter frequency
Δ	: displaced volume of ship

References

- Fang, M. C. (1985) Relative elevation and pressure distribution of a two-dimensional catamaran ship in beam waves. *Journal of SNAME*, **4**, 71-77.
- Fang, M. C. (1987) *An Analysis on Seakeeping of SWATH in Waves*. NSC 76-0403-E006-01 Report, National Science Council, R.O.C., Taipei, R.O.C.
- Fang, M. C. (1988) The motions of SWATH ship in waves. *Journal of Ship Research*, **32**(4), 238-245.
- Kim, C. H. (1976) Motions and loads of a catamaran ship of arbitrary ship of arbitrary shape in a seaway. *Journal of Hydronautics*, **10**(1), 8-17.
- Kim, C. H., F. S. Chou, and D. Tein (1980) Motions and hydrodynamic loads of a ship advancing in oblique waves. *Trans., SNAME*, **88**, 225-256.
- Kim, C. H. (1972) *The Hydrodynamic Interaction Between Two Cylindrical Bodies Floating in Beam Seas*. Report No. SIT-OE-72-10, Stevens Institute of Technology, Hoboken, NJ, U.S.A.
- Lee, C. M., H. D. Jones, and R. M. Curphey (1973) Prediction of motion and hydrodynamic loads of catamarans. *Marine Technology*, **10**(4), 392-405.
- Lee, C. M. and R. M. Curphey (1977) Prediction of motion, stability and wave loads of small-water-area, twin-hull ships. *SNAME Transactions*, **85**, 94-130.
- Reilly, E. T., Y. S. Shin, and H. Kotte (May, 1988) A prediction of structural load and response of a SWATH ship in waves. *Naval Engineers Journal*, 251-264.
- Yi, S. F. (1994) *The Analysis of Motions and Wave Loads for a Catamaran Ship in Waves*. Master Thesis. National Cheng-Kung University, Tainan, Taiwan, R.O.C.
- Wahab, R., C. Pritchett, and L. C. Ruth (1971) On the behavior of the ASR catamaran in waves. *Marine Technology*, **8**, 334-360.

雙體船之波浪負荷預測法

方銘川* 李銘霖*；余盛富**

*成功大學造船及船舶機械工程研究所

**高雄海事專科學校造船科

摘 要

本文係以截片理論為基礎，分析雙體船在規則波中運動時，其橫甲板所承受的波浪荷重。由於雙體船的波浪荷重與其運動及作用在各截面的流體動力有密切關係，本文首先說明船體運動的數學模式以及流體動力的求法，其中流體動力尚需考慮兩船殼間的交互影響。利用切取自由體的觀念，將上述所有作用在船殼上的波浪力、流體動力及船體的慣性力，在雙體船的橫甲板跨距中央處，求其合力及合力矩，此即波浪荷重。目前最常用的方法有一般方法及簡化法，本文綜合以上兩種方法再提出另一種改進的計算方法。即將簡化的方法加入前述一般法所考慮的實際船型在不同截面的形狀以及縱搖與平擺運動對波浪荷重的影響而發展出一種混合法。

本文以ASR雙體船為數值計算模型，以自行開發之一般法及混合法的電算程式來進行其波浪荷重計算，並將所得數值與現有文獻之實驗數據及簡化法的計算結果相比對，可明顯看出混合法的計算值較另二法所得值更接近實驗結果，而且更有效率。因此可提供雙體船波浪荷重分析一項有力的計算工具。